

Electron Transfer in Proteins

# Control of the Electronic Ground State on an Electron-Transfer Copper Site by Second-Sphere Perturbations\*\*

Marcos N. Morgada, Luciano A. Abriata, Ulises Zitare, Damian Alvarez-Paggi, Daniel H. Murgida, and Alejandro J. Vila\*

**Abstract:** The  $Cu_A$  center is a dinuclear copper site that serves as an optimized hub for long-range electron transfer in heme-copper terminal oxidases. Its electronic structure can be described in terms of a  $\sigma_u^*$  ground-state wavefunction with an alternative, less populated ground state of  $\pi_u$  symmetry, which is thermally accessible. It is now shown that second-sphere mutations in the  $Cu_A$  containing subunit of *Thermus thermophilus*  $ba_3$  oxidase perturb the electronic structure, which leads to a substantial increase in the population of the  $\pi_u$  state, as shown by different spectroscopic methods. This perturbation does not affect the redox potential of the metal site, and despite an increase in the reorganization energy, it is not detrimental to the electron-transfer kinetics. The mutations were achieved by replacing the loops that are involved in protein-protein interactions with cytochrome *c*, suggesting that transient protein binding could also elicit ground-state switching in the oxidase, which enables alternative electron-transfer pathways.

The  $Cu_A$  center is a binuclear copper site that acts as the electron entry port in terminal heme-copper oxidases and in  $N_2O$  reductases.<sup>[1]</sup> The high efficiency of this metal site in long-range intra- and intermolecular electron transfer (ET) has been attributed to its unusual coordination features, which ensure a low reorganization energy ( $\lambda$ ) and an electronic structure that is poised to meet the physiological requirements.<sup>[2]</sup> The two copper ions are bridged by two Cys ligands forming a nearly planar  $\{Cu_2S_2\}$  diamond core, with two additional His residues and two weak axial ligands (a Met and a backbone carbonyl moiety; Figure 1).<sup>[1,3]</sup> The oxidized,

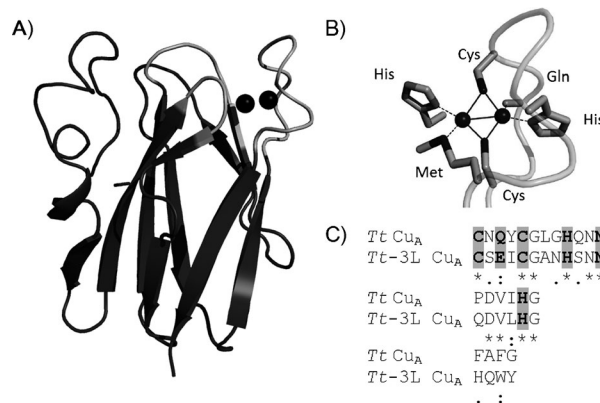


**Figure 1.** A) Structure of wild-type Tt  $Cu_A$  (PDB 2CUA). The loops that are replaced in the Tt-3L  $Cu_A$  chimera are shown in light gray. B) Structure of the  $Cu_A$  site highlighting the metal ligands. C) Alignment of the replaced loops shows that the metal ligands and the loop lengths are preserved in the Tt-3L  $Cu_A$  mutant.

resting-state  $Cu_A$  center is a fully delocalized mixed-valence pair<sup>[4]</sup>  $Cu^{1.5+}Cu^{1.5+}$  with one electron delocalized mostly within the  $\{Cu_2S_2\}$  core.<sup>[5]</sup> The electronic structure can be described by a  $\sigma_u^*$  ground-state wavefunction, that is, it involves an anti-bonding  $\sigma$  interaction between the two copper ions. An alternative ground state of  $\pi_u$  symmetry with higher energy is partially populated at room temperature and rapidly interconverts with the  $\sigma_u^*$  state.<sup>[5c,d,6]</sup> The role of the two states in electron transfer has been a matter of intense debate.<sup>[6c,7]</sup>

We have recently shown that both the redox potential of the  $Cu_A$  site and the  $\sigma_u^*/\pi_u$  energy gap can be tuned by replacing the native Met residue with different axial ligands. The population of the  $\pi_u$  level, which is typically < 5% in the resting-state protein, increases to 30% when a His residue is introduced as the axial ligand.<sup>[7b,8]</sup> The  $\pi_u$  state displays a higher reorganization energy in this mutant, which is compensated by a larger superexchange coupling, therefore enabling efficient electron transfer. These findings led us to propose that the availability of two alternative ground states could be exploited by the oxidase to switch between two ET pathways.<sup>[7b]</sup> However, ligand mutations are expected to elicit significant changes in metal sites, which might not be of biochemical relevance. Last but not least, in contrast to type 1 (blue) copper sites,  $Cu_A$  displays a fully conserved ligand set in all known  $Cu_A$  containing proteins.<sup>[2b]</sup> This observation is in line with their functional requirements: All  $Cu_A$  sites display roughly the same redox potentials, whereas type 1 centers are meant to accept and deliver electrons in different ET chains,

[\*] M. N. Morgada, Dr. L. A. Abriata,<sup>[†]</sup> Prof. A. J. Vila  
Instituto de Biología Molecular y Celular de Rosario (IBR)  
Departamento de Química Biológica  
Facultad de Ciencias Bioquímicas y Farmacéuticas  
Universidad Nacional de Rosario, CONICET  
Ocampo y Esmeralda, Rosario (Argentina)  
E-mail: vila@ibr-conicet.gov.ar

U. Zitare, Dr. D. Alvarez-Paggi, Prof. D. H. Murgida  
Departamento de Química Inorgánica, Analítica y Química Física—  
INQUIMAE, Facultad de Ciencias Exactas y Naturales  
Universidad de Buenos Aires—CONICET (Argentina)

[†] Current address: Laboratory of Biomolecular Modeling and Swiss  
Institute of Bioinformatics  
École Polytechnique Fédérale de Lausanne/EPFL (Switzerland)

[\*\*] We thank CONICET and ANPCyT for funding, Dr. A. Gallo and Dr. L. Sorace (University of Firenze) for the acquisition of the EPR spectra, and Dr. C. Brondino for helpful discussions.

Supporting information for this article is available on the WWW  
under <http://dx.doi.org/10.1002/anie.201402083>.

and their redox potentials need to be modulated depending on their partners.<sup>[9]</sup> This tuning is determined by the strength of the interaction between the copper center and the axial ligand, the length of the protein loops that contain several copper ligands, and by the interactions with second-sphere residues.<sup>[10]</sup> Instead, Cu<sub>A</sub> centers display fully conserved metal ligands and loop lengths,<sup>[11]</sup> with changes being limited to non-ligand residues, that is, second-sphere interactions.

Herein, we report the design of a chimeric protein in the scaffold of the Cu<sub>A</sub> containing domain from *Thermus thermophilus* ba<sub>3</sub> oxidase, in which the three loops that define the nearby environment of the metal site were replaced by those from a homologous eukaryotic domain (Figure 1; see also the Supporting Information, Figure S1). This chimera, which we named *Tt*-3L Cu<sub>A</sub>, shows perturbed spectroscopic features, which are due to a large increase in the population of the  $\pi_u$  level. This phenomenon was achieved with a conserved ligand set, which contributes to maintaining the redox potential of the native site. Therefore, switching between the two alternative ground states can be elicited by second-sphere perturbations that preserve the functional thermodynamic requirements.

The reduction potential ( $E^\circ$ ) of the *Tt*-3L Cu<sub>A</sub> chimera was determined by cyclic voltammetry (CV) of protein samples in solution to be  $281 \pm 8$  mV, which is similar to the value of the wild-type (WT *Tt* Cu<sub>A</sub>) protein within experimental error, thereby indicating that the ligand set is essential for determining the  $E^\circ$  value of the site. The ET reorganization free energy ( $\lambda$ ) of *Tt*-3L Cu<sub>A</sub> was obtained from CV experiments that were performed on protein samples adsorbed on gold electrodes coated with biocompatible films. The rate constant of heterogeneous ET ( $k_{ET}$ ) was determined using the Laviron working curve as a function of temperature between 5 and 39 °C (Figure S2), yielding a  $\lambda$  value of  $0.58 \pm 0.05$  eV, which is higher than the value of 0.4 eV that was determined for WT *Tt* Cu<sub>A</sub>.

The absorption spectrum of the *Tt*-3L Cu<sub>A</sub> chimera in the UV/Vis range is significantly perturbed in comparison with that of the WT protein (Figure 2A). Even though the characteristic purple color is retained, the intensity ratio of the two Cys–copper ligand-to-metal charge transfer (LMCT) transitions at 18 700 and 21 270 cm<sup>-1</sup> is altered.<sup>[5a,6d]</sup> An absorption feature at approximately 27 000 cm<sup>-1</sup> has experienced a substantial increase in intensity, which indicates a larger population of the  $\pi_u$  ground state, as shown for M160H-Cu<sub>A</sub> (Figure 2A).<sup>[7b]</sup> In the near-IR region, the  $\psi \rightarrow \psi^*$  intervalence band has slightly shifted from 12 650 to 12 570 cm<sup>-1</sup> and retained a similar extinction coefficient. This absorption band reflects the electronic coupling between the two copper ions,  $H_{AB}$ , which is only reduced by 80 cm<sup>-1</sup>, suggesting that the short Cu–Cu distance is retained in this variant (Table S1).<sup>[6b]</sup> The EPR spectrum of *Tt*-3L Cu<sub>A</sub> recorded at 5 K is typical for Cu<sub>A</sub> centers (Figure 2B). Overall, these data support an increased population of the  $\pi_u$  ground state.

NMR spectroscopy is the technique of choice for directly studying the equilibrium between the  $\sigma_u^*$  and  $\pi_u$  ground states in Cu<sub>A</sub> centers at physiologically relevant temperatures, allowing an estimation of the energy gap between these two

states.<sup>[5c,d,7b,8,12]</sup> The <sup>1</sup>H NMR spectrum of *Tt*-3L Cu<sub>A</sub> displays four hyperfine-shifted signals between 150 and 300 ppm, which correspond to the  $\beta$  protons of the Cys ligands (Figure S3). Resonances that are due to the His ligands are located between 15 and 50 ppm. Three additional proton resonances, namely those of the two  $\alpha$  hydrogen atoms of the Cys ligand and the NH moiety of Gly 115, could also be identified and assigned. Direct-detected <sup>13</sup>C NMR spectroscopy is particularly useful in this system, as the larger differences in chemical shift and the lower gyromagnetic ratio of the <sup>13</sup>C nuclei make it less sensitive to paramagnetism.<sup>[13]</sup> Resonances were assigned by the combined use of 1D and 2D <sup>1</sup>H and <sup>13</sup>C NMR spectra, following an already described strategy.<sup>[7b,8]</sup>

Carbon resonances from the His ligands are similar to the corresponding resonances for the WT protein, whereas axial-ligand mutations elicited differences between the two His residues (Figure 2C).<sup>[7b]</sup> Instead, the patterns of the <sup>1</sup>H and <sup>13</sup>C resonances from the Cys ligands were perturbed and could be employed as a probe for the relative populations of the  $\sigma_u^*$  and  $\pi_u$  states.<sup>[8]</sup> The S153–S149–C $\beta$ 149–C $\alpha$ 149 dihedral angle allows minimal electron spin density on the  $\alpha$  carbon atom of Cys149 in the  $\sigma_u^*$  state and a large spin delocalization in the  $\pi_u$  state.<sup>[8]</sup> This resonance has shifted from 295 ppm for the WT protein to 539 ppm for *Tt*-3L Cu<sub>A</sub>, which clearly discloses a large population of the  $\pi_u$  state in the mutant (Figure 2C). Analysis of the temperature dependence of the <sup>1</sup>H and <sup>13</sup>C chemical shifts by assuming a two-state model with a Boltzmann distribution yields an energy gap of  $240 \pm 87$  cm<sup>-1</sup>, which corresponds to a 74:26( $\pm$ 7) ratio for the population of the  $\sigma_u^*$  and  $\pi_u$  states at 298 K, compared to a 95:5( $\pm$ 3) ratio for WT Cu<sub>A</sub> (Table S3).

Such a low energy difference is expected to introduce temperature dependence for the absorption spectra in a physiologically relevant temperature range. We recorded the absorption spectra of *Tt*-3L Cu<sub>A</sub> in the 276–312 K temperature range in aqueous solution, avoiding perturbations that arise from the use of solvent mixtures or sample freezing. The series of spectra show four well-defined isobestic points at 22 000, 17 000, 14 000, and 11 000 cm<sup>-1</sup>, disclosing an equilibrium between two species with distinct electronic states (Figure 3). The intensity of the band at 27 000 cm<sup>-1</sup> clearly decreases at lower temperatures, which is in agreement with the expected reduced population of the  $\pi_u$  state. The differences in the  $\psi \rightarrow \psi^*$  intervalence band are minor, which is in line with the observation that this feature is not substantially perturbed in this mutant. A similar effect can be observed in the electronic spectrum of mutant M160H, which presents a comparable energy gap (200 cm<sup>-1</sup>; Figure S4). The temperature dependence of the absorption spectra provides further evidence for the increased population of the  $\pi_u$  ground state in these two mutants, as well as for its equilibrium regime with the  $\sigma_u^*$  state.

In summary, these data show that 1) outer-sphere perturbations can propagate towards the first ligand sphere, which leads to an increase in the population of the  $\pi_u$  ground state, and that 2) the  $\pi_u$  state is active for electron transfer. In contrast with previous studies,<sup>[7b]</sup> this has been achieved without changing the identity of the copper ligands. As

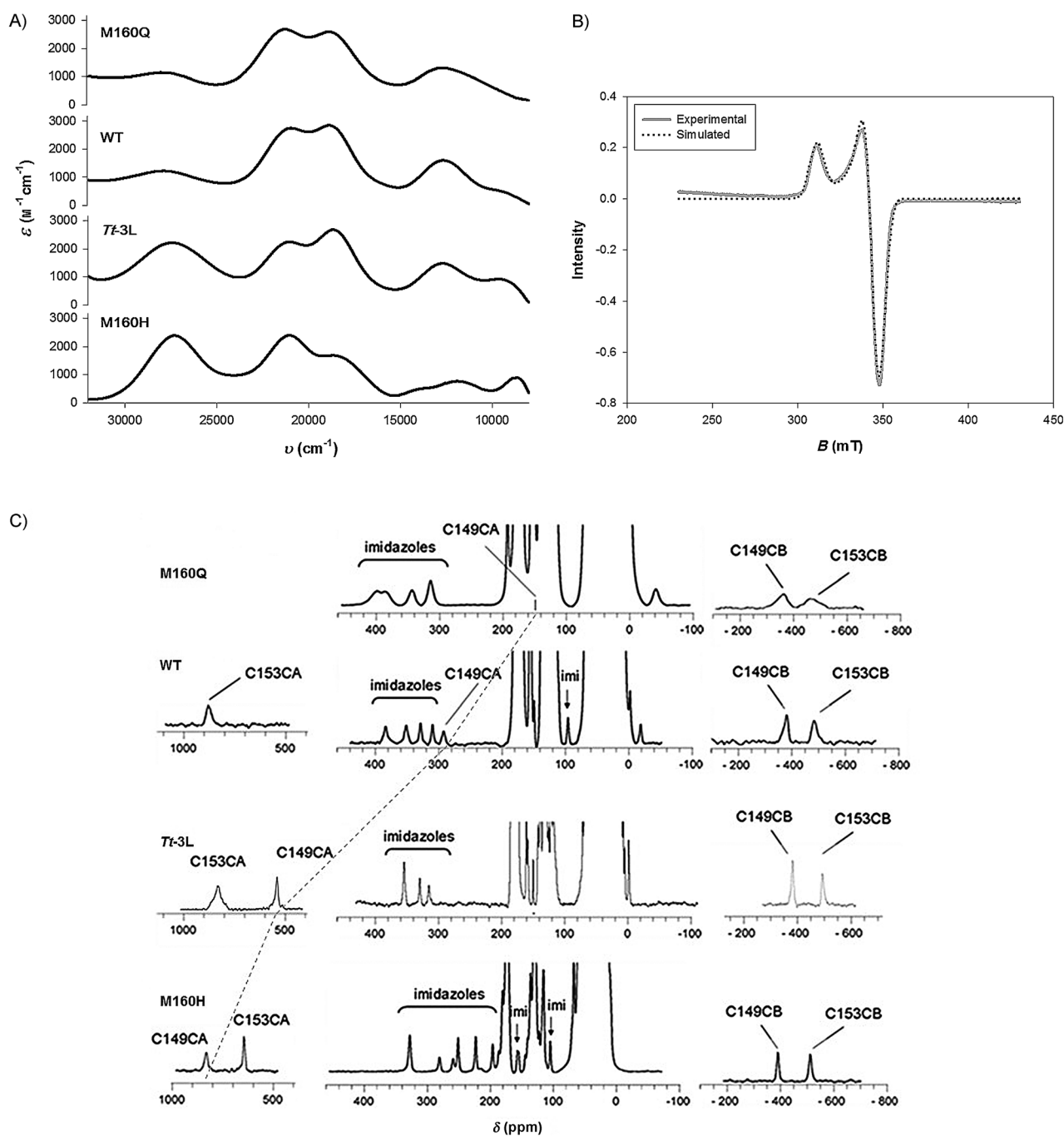


**Figure 2.** A) Absorption spectra of the  $\text{Cu}_A$  mutants. B) Experimental and simulated EPR spectrum of *Tt*-3L  $\text{Cu}_A$ . C)  $^{13}\text{C}$  NMR spectra of the  $\text{Cu}_A$  mutants. The spectral position of the signal from C149CA is a probe of the energy gap between the  $\sigma_u^*$  and  $\pi_u$  states.

a result, this perturbation does not alter the redox potential of the  $\text{Cu}_A$  site. Therefore, the electronic structure of the  $\text{Cu}_A$  site can be tuned by second-sphere perturbations, which enable the transient population of alternative ground states without a significant energetic cost while preserving the thermodynamic features (redox potential). Regarding the ET kinetics, the population of the  $\pi_u$  ground state leads to an increase in the reorganization energy from 0.4 to 0.58 eV. A similar increase in  $\lambda$ , which nevertheless was not detrimental for the ET rate, has recently been reported for the M160H-

$\text{Cu}_A$  mutant. It is remarkable that the  $\sigma_u^*-\pi_u$  energy gap is comparable in these mutants (240 vs. 200  $\text{cm}^{-1}$ ), which gives rise to similar relative populations of these two states under equilibrium conditions. In both cases, the increase in reorganization energy does not exert a negative impact on the ET rates, suggesting that it is compensated for by an increase in the superexchange coupling. Indeed, these  $\lambda$  values are still lower than those reported for type 1 copper centers (0.7–0.8 eV),<sup>[14]</sup> which confirms that they are compatible with efficient biological electron transfer.

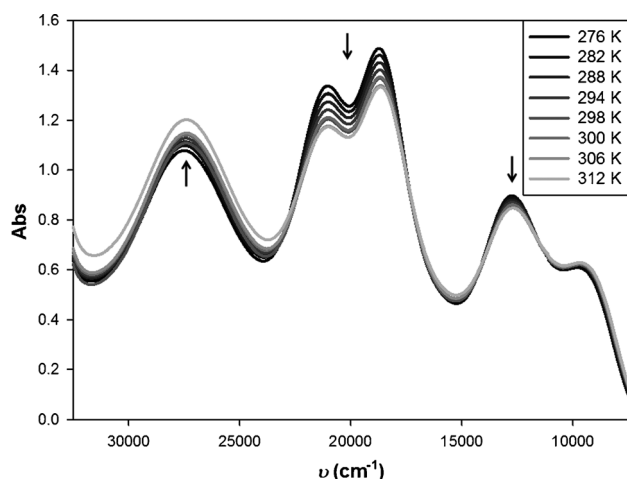


**Figure 3.** Temperature dependence of the absorption spectrum of Tt-3L Cu<sub>A</sub>.

The availability of these two alternative ground states could be employed by the oxidase to switch between two electron-transfer pathways.<sup>[7b]</sup> Given that subunit II is anchored to the membrane, this mechanism would allow switching without conformational reorientation. The three loops that were replaced in this chimera are involved in the binding of the natural electron donor, cytochrome *c*<sub>552</sub>, to subunit II of the oxidase, as shown by NMR experiments.<sup>[15]</sup> Therefore, perturbations in these loops that are induced by transient cytochrome binding could favor the  $\pi_u$  ground state, enabling different ET pathways in the enzyme.<sup>[7b]</sup> The study of the inter-protein ET reaction with the natural redox partner, which involves disentangling the diffusion, reorientation, and electron-transfer steps from the obtained kinetics data, is currently underway. Similar loop replacements to those presented here for type 1 sites revealed that changes in the loop length, but not in the loop sequence, can alter the electronic structure of the metal center.<sup>[9a]</sup> Therefore, even though the Cu<sub>A</sub> site is more rigid than type 1 centers, it possesses an electronic structure that is tunable by subtle, transient perturbations. The electronic structure of this metal site should be described by considering both ground states and their differential role in long-range electron transfer.

## Experimental Section

**Preparation of protein samples:** Unlabeled and uniformly labeled proteins were expressed from pET9ACu<sub>A</sub>WTT9 (KanR) in *E. coli* BL21(DE3) growing in either rich LB medium or M9 minimal medium supplemented with labeled or unlabeled ammonium sulfate (1.2 g L<sup>-1</sup>, 99% <sup>15</sup>N when labeled) and glucose (4 g L<sup>-1</sup>, 99% <sup>13</sup>C when labeled), respectively, according to the desired labeling scheme. Typical yields were approximately 20 mg L<sup>-1</sup> and 30 mg L<sup>-1</sup> for labeled and unlabeled samples, respectively. Purification of the proteins from cell lysates was done as described elsewhere.<sup>[16]</sup> Protein samples for NMR experiments were prepared in phosphate buffer (100 mM, pH 6) with KCl (100 mM) in either 10% or 100% D<sub>2</sub>O as required for each experiment, and concentrated to 250–300  $\mu$ L of 0.6–1 mM protein concentration.

**NMR spectroscopy:** NMR experiments were carried out on a Bruker Avance II Spectrometer operating at 600.13 MHz (<sup>1</sup>H frequency). <sup>1</sup>H NMR spectra were acquired with a triple-resonance (TXI) probe head. <sup>1</sup>H NMR spectra in the 35/–10 ppm region were observed with a  $\pi/2$  pulse preceded by presaturation of the water signal, on a spectral window of approximately 48 kHz, and with a total recycle time of ca. 300 ms. <sup>1</sup>H NMR spectra aimed at the observation of the broad  $\beta$ -hydrogen signals were acquired with a SuperWEFT pulse sequence<sup>[17]</sup> on a spectral window of approximately 360 kHz, with a total recycle delay of approximately 40 ms and variable intermediate delays. <sup>1</sup>H, <sup>13</sup>C and <sup>1</sup>H, <sup>15</sup>N HMQC experiments were acquired on spectral widths of approximately 50 kHz in the 1H dimension (1024 points) and approximately 100 kHz in the indirect dimension (128 points). The delay for coherence transfer was set to the average *T*<sub>2</sub> of the involved <sup>1</sup>H signals, that is, about 2 ms, and the relaxation delay was set to approximately 30 ms.<sup>[18]</sup> Several experiments were carried out setting the frequency of the heteronucleus at different offsets.

<sup>13</sup>C NMR spectra were acquired with a broadband observe (BBO) probehead tuned at the proper frequency, using an excitation pulse of 6.9  $\mu$ s at 88.67 W. Inverse gated decoupling was applied during the acquisition of <sup>13</sup>C NMR spectra. For <sup>13</sup>C NMR experiments, the carrier frequency was set to 800, 300, or –500 ppm depending on which signals were being studied. The spectral window and delays also varied in each experiment, which resulted in total recycle times of approximately 35 ms for the acquisition of signals around 800 and –500 ppm, and approximately 300 ms for those near the diamagnetic region. No further signals were detected when the carrier was moved to different frequency offsets.

**Fitting of the temperature dependence data:** The temperature dependence data were fit to a two-state model using the approach described by Shokhirev and Walker,<sup>[12]</sup> which calculates the contact contribution to the chemical shift for each data point and fits all data at once to the following equation:

$$\delta_{\text{contact},k} = \frac{1}{T} \frac{f_{k,1} + f_{k,2} e^{-\frac{\Delta E}{k_B T}}}{1 + e^{-\frac{\Delta E}{k_B T}}} \quad (1)$$

Fitting the data to this equation yields  $f_{k,i}$ , which is the contribution of nucleus *k* to the contact shift in the state *i* (*i* = 1 for the ground state, *i* = 2 for the excited state), and  $\Delta E$ , the energy gap between the two states.

**EPR spectroscopy:** EPR spectra of oxidized Tt-3L Cu<sub>A</sub> in phosphate buffer (100 mM) at pH 6 with KCl (100 mM) and glycerol (10%) were measured on a Bruker Elexsys E500 spectrometer equipped with an X-band microwave bridge (microwave frequency, 9.45 GHz) and a unit for temperature control (ER 4131 VT). EPR parameters: sample temperature: 5 K; microwave frequency: 9.45 GHz; microwave power: 5 mW; modulation frequency: 9387691 GHz; modulation amplitude: 2500 G, time constant: 167 ms. The EPR data were fitted using Easyspin.<sup>[19]</sup>

**Cyclic voltammetry in solution:** Cyclic voltammetry was performed with a Gamry REF600 potentiostat in a cell equipped with a polycrystalline gold bead working electrode, a platinum wire auxiliary electrode, and a Ag/AgCl reference electrode. Gold working electrodes were coated with a self-assembled monolayer by overnight incubation in an ethanolic solution of HS(CH<sub>2</sub>)<sub>6</sub>OH (1 mM). After thorough rinsing with ethanol and deionized water, the coated electrodes were placed in the electrochemical cell, which contained a protein solution (300  $\mu$ M; in acetate buffer (10 mM), KNO<sub>3</sub> (500 mM), pH 4.6). The pH was adjusted by the addition of HClO<sub>4</sub> or KOH, which was followed by two minutes of equilibration.

**Protein film voltammetry:** Gold working electrodes were coated with a mixed self-assembled monolayer by overnight incubation in an ethanolic solution of HS(CH<sub>2</sub>)<sub>5</sub>CH<sub>3</sub> (2 mM) and HS(CH<sub>2</sub>)<sub>6</sub>OH (3 mM). After thorough rinsing with ethanol and deionized water, the coated electrodes were incubated in a protein solution (100  $\mu$ M, in



acetate buffer (10 mM), pH 4.6) for two hours for protein adsorption and then transferred to the electrochemical cell. Measurements were performed in acetate buffer (10 mM) containing KNO<sub>3</sub> (200 mM) as the supporting electrolyte. The temperature was held constant during the measurements by controlling the temperature of a water jacket cell that was coupled to a circulating thermostat.

Received: February 4, 2014

Revised: February 24, 2014

Published online: April 28, 2014

**Keywords:** electron transfer · electronic structure · metalloproteins · NMR spectroscopy · second-shell perturbations

- [1] H. Beinert, *Eur. J. Biochem.* **1997**, *245*, 521–532.
- [2] a) E. I. Solomon, X. Xie, A. Dey, *Chem. Soc. Rev.* **2008**, *37*, 623–638; b) H. B. Gray, B. G. Malmström, R. J. Williams, *J. Biol. Inorg. Chem.* **2000**, *5*, 551–559; c) B. E. Ramirez, B. G. Malmström, J. R. Winkler, H. B. Gray, *Proc. Natl. Acad. Sci. USA* **1995**, *92*, 11949–11951.
- [3] a) P. A. Williams, N. J. Blackburn, D. Sanders, H. Bellamy, E. A. Stura, J. A. Fee, D. E. McRee, *Nat. Struct. Biol.* **1999**, *6*, 509–516; b) J. Salgado, G. C. Warmerdam, L. Bubacco, G. W. Canters, *Biochemistry* **1998**, *37*, 7378–7389; c) T. Soulimane, G. Buse, G. P. Bourenkov, H. D. Bartunik, R. Huber, M. E. Than, *EMBO J.* **2000**, *19*, 1766–1776; d) M. Kelly, P. Lappalainen, G. Talbo, T. Haltin, J. van der Oost, M. Saraste, *J. Biol. Chem.* **1993**, *268*, 16781–16787.
- [4] P. M. H. Kroneck, W. E. Antholine, J. Riester, W. G. Zumft, *FEBS Lett.* **1988**, *242*, 70–74.
- [5] a) J. A. Farrar, F. Neese, P. Lappalainen, P. M. H. Kroneck, M. Saraste, W. G. Zumft, A. J. Thompson, *J. Am. Chem. Soc.* **1996**, *118*, 11501–11514; b) F. Neese, W. G. Zumft, W. A. Antholine, P. M. H. Kroneck, *J. Am. Chem. Soc.* **1996**, *118*, 8692–8699; c) I. Bertini, K. L. Bren, A. Clemente, J. A. Fee, H. B. Gray, C. Luchinat, B. G. Malmström, J. H. Richards, D. Sanders, C. E. Slutter, *J. Am. Chem. Soc.* **1996**, *118*, 11658–11659; d) J. Salgado, H. R. Jimenez, J. M. Moratal Mascarell, S. Kroes, G. C. M. Warmerdam, G. W. Canters, *Biochemistry* **1996**, *35*, 1810–1819.
- [6] a) S. DeBeer George, M. Markus, H. Wang, S. P. Cramer, Y. Lu, W. B. Tolman, B. Hedman, K. O. Hodgson, E. I. Solomon, *J. Am. Chem. Soc.* **2001**, *123*, 5757–5767; b) D. R. Gamelin, D. W. Randall, M. T. Hay, R. P. Houser, T. C. Mulder, G. W. Canters, S. De Vries, W. B. Tolman, E. I. Solomon, *J. Am. Chem. Soc.* **1998**, *120*, 5246–5263; c) M. H. Olsson, U. Ryde, *J. Am. Chem. Soc.* **2001**, *123*, 7866–7876; d) X. Xie, S. I. Gorelsky, R. Sarangi, D. K. Garner, H. J. Hwang, K. O. Hodgson, B. Hedman, Y. Lu, E. I. Solomon, *J. Am. Chem. Soc.* **2008**, *130*, 5194–5205.
- [7] a) S. I. Gorelsky, X. Xie, Y. Chen, J. A. Fee, E. I. Solomon, *J. Am. Chem. Soc.* **2006**, *128*, 16452–16453; b) L. A. Abriata, D. Alvarez-Paggi, G. N. Ledesma, N. J. Blackburn, A. J. Vila, D. H. Murgida, *Proc. Natl. Acad. Sci. USA* **2012**, *109*, 17348–17353; c) M. L. Tsai, R. G. Hadt, N. M. Marshall, T. D. Wilson, Y. Lu, E. I. Solomon, *Proc. Natl. Acad. Sci. USA* **2013**, *110*, 14658–14663; d) M. Gennari, J. Pecaut, S. DeBeer, F. Neese, M. N. Collomb, C. Duboc, *Angew. Chem.* **2011**, *123*, 5780–5784; *Angew. Chem. Int. Ed.* **2011**, *50*, 5662–5666.
- [8] L. A. Abriata, G. N. Ledesma, R. Pierattelli, A. J. Vila, *J. Am. Chem. Soc.* **2009**, *131*, 1939–1946.
- [9] a) E. I. Solomon, R. K. Szilagy, G. S. DeBeer, L. Basumallick, *Chem. Rev.* **2004**, *104*, 419–458; b) A. J. Vila, C. O. Fernandez in *Handbook of Metalloproteins* (Eds.: I. Bertini, A. Sigel, H. Sigel), Marcel Dekker, New York, **2001**.
- [10] a) C. Dennison, *Dalton Trans.* **2005**, 3436–3442; b) N. M. Marshall, D. K. Garner, T. D. Wilson, Y. G. Gao, H. Robinson, M. J. Nilges, Y. Lu, *Nature* **2009**, *462*, 113–116; c) R. G. Hadt, N. Sun, N. M. Marshall, K. O. Hodgson, B. Hedman, Y. Lu, E. I. Solomon, *J. Am. Chem. Soc.* **2012**, *134*, 16701–16716; d) R. Sarangi, S. I. Gorelsky, L. Basumallick, H. J. Hwang, R. C. Pratt, T. D. Stack, Y. Lu, K. O. Hodgson, B. Hedman, E. I. Solomon, *J. Am. Chem. Soc.* **2008**, *130*, 3866–3877; e) K. M. Lancaster, G. S. DeBeer, K. Yokoyama, J. H. Richards, H. B. Gray, *Nat. Chem.* **2009**, *1*, 711–715; f) K. M. Lancaster, *Struct. Bonding (Berlin)* **2011**, *142*, 119–153.
- [11] L. A. Abriata, *Acta Crystallogr. Sect. D* **2012**, *68*, 1223–1231.
- [12] N. V. Shokhirev, F. A. Walker, *J. Phys. Chem.* **1995**, *99*, 17795–17804.
- [13] a) W. Bermeil, I. Bertini, I. C. Felli, R. Kummerle, R. Pierattelli, *J. Am. Chem. Soc.* **2003**, *125*, 16423–16429; b) F. Arnesano, L. Banci, I. Bertini, I. C. Felli, C. Luchinat, A. R. Thompson, *J. Am. Chem. Soc.* **2003**, *125*, 7200–7208.
- [14] A. J. Di Bilio, M. G. Hill, N. Bonander, B. G. Karlsson, R. M. Villahermosa, B. G. Malmström, J. R. Winkler, H. B. Gray, *J. Am. Chem. Soc.* **1997**, *119*, 9921–9922.
- [15] L. Muresanu, P. Pristovsek, F. Lohr, O. Maneg, M. D. Mukrasch, H. Ruterjans, B. Ludwig, C. Lucke, *J. Biol. Chem.* **2006**, *281*, 14503–14513.
- [16] a) C. E. Slutter, D. Sanders, P. Wittung, B. G. Malmström, R. Aasa, J. H. Richards, H. B. Gray, J. A. Fee, *Biochemistry* **1996**, *35*, 3387–3395; b) C. O. Fernández, J. A. Cricco, C. E. Slutter, J. H. Richards, H. B. Gray, A. J. Vila, *J. Am. Chem. Soc.* **2001**, *123*, 11678–11685.
- [17] T. Inubushi, E. D. Becker, *J. Magn. Reson.* **1983**, *51*, 128–133.
- [18] L. Banci, I. Bertini, R. Pierattelli, A. J. Vila, *Inorganic Chemistry* **1994**, *33*, 4338–4343.
- [19] S. Stoll, A. Schweiger, *J. Magn. Reson.* **2006**, *178*, 42–55.